

The Hermite correction method for nonadiabatic transitions

Satrajit Adhikari and Gert D. Billing

Citation: *The Journal of Chemical Physics* **111**, 48 (1999); doi: 10.1063/1.479252

View online: <http://dx.doi.org/10.1063/1.479252>

View Table of Contents: <http://scitation.aip.org/content/aip/journal/jcp/111/1?ver=pdfcov>

Published by the [AIP Publishing](#)

Articles you may be interested in

[Control scheme of nonadiabatic transitions with the dynamical shift of potential curve crossing](#)

J. Chem. Phys. **140**, 244115 (2014); 10.1063/1.4884784

[A semiclassical model for the calculation of nonadiabatic transition probabilities for classically forbidden transitions](#)

J. Chem. Phys. **130**, 054107 (2009); 10.1063/1.3066595

[Stark slowing asymmetric rotors: Weak-field-seeking states and nonadiabatic transitions](#)

J. Chem. Phys. **123**, 194305 (2005); 10.1063/1.2112787

[Phase corrected higher-order expression for surface hopping transition amplitudes in nonadiabatic scattering problems](#)

J. Chem. Phys. **119**, 11048 (2003); 10.1063/1.1622662

[Direct observation of nonadiabatic transitions in Na+rare-gas differential optical collisions](#)

J. Chem. Phys. **111**, 2853 (1999); 10.1063/1.479566



The Hermite correction method for nonadiabatic transitions

Satrajit Adhikari and Gert D. Billing^{a)}

Department of Chemistry, H.C.Ørsted Institute, University of Copenhagen, DK-2100 Ø, Denmark

(Received 12 March 1999; accepted 6 April 1999)

We have performed molecular dynamics simulations on a system where electronic transitions are allowed anywhere in configuration space among any number of coupled states. A classical path theory based on the Hermite correction to the Gaussian wave packet expansion, proposed by Gert D. Billing [J. Chem. Phys. **107**, 4286 (1997)] has been used. The calculations are carried out on the same model used by J. C. Tully [J. Chem. Phys. **93**, 1061 (1990)] and the transition probabilities agree well with corresponding exact quantum mechanical results. © 1999 American Institute of Physics. [S0021-9606(99)01125-3]

I. INTRODUCTION

The motivation for deriving the classical path (CP) theory from first principles was to achieve a systematic way of going from the full classical limit to an exact theory and thereby to incorporate the quantum effects in a systematic way.¹⁻³ In the present article, we have studied systems which have nonadiabatic transitions and the equations of motion are derived from the Schrödinger equation using a Gauss–Hermite basis set. This derivation reveals that some variables appear as “classical” quantities while others are quantum mechanical. The equations of motion for the classical variables are governed by an effective potential averaged over the quantum ones. In order to formulate the classical path equations from first principles in the present perspective, we can introduce an approximation concerning the form of the basis function, $\Phi_0(x,t)$, namely that it is a Gaussian wave packet (GWP). Finally, using a rigorous approach based on the introduction of a Hermite correction to the GWP, it is easy to improve the CP theory and approach an exact theory. The basis functions have, therefore, been denoted as a Gauss–Hermite basis set. More explicitly, the wave function, $\psi(x,t)$, is expanded using the Gauss–Hermite basis, $\Phi_n(x,t)$, which has two important properties: (i) They form an orthonormal basis. (ii) The ground state of the basis is the Gaussian wave packet (GWP).

Though concepts behind our present method are related to the Gaussian wave packet theory by Heller,⁴ the minimum error method (MEM)⁵ or the trajectory based “spawning” method by Levine and co-workers,⁶ these methods are developed by using Gaussian basis functions only. Since the Gaussian basis set is nonorthogonal, evaluation of overlap integrals and inversion of matrices need to be performed in each time step. The present method avoids these numerically cumbersome steps due to the use of an orthogonal basis set. The method is furthermore related to the time-dependent multiconfiguration Hartree method.⁷

The time-dependent basis set ($\Phi_n(x,t)$) used to correct the primitive classical path theory can basically offer a multiconfiguration self-consistent field (MCSCF) method.^{2,8}

Though the Gauss–Hermite basis set has also been used before,⁹⁻¹⁵ the way of propagating the classical variables is different from those proposed earlier. Again, in the present methodology, the generalization to multidimensional multisurface systems is rather straightforward compared to earlier approaches.

In this article, we have studied two one-dimensional two-state models¹⁶ where nonadiabatic effects play a significant role in the electronic transition processes. As the Gauss–Hermite basis is complete and exact, the method should be able to mimic the quantum effects (electronic transitions). The initial wave function is taken to be a GWP on the lower adiabatic surface. As a GWP covers a certain range in momentum space, it is possible to extract the information on the transition probabilities in an energy range with a single propagation. The probability, at a particular energy, is obtained as the ratio of outgoing and incoming flux components calculated at that energy. The incoming and outgoing fluxes are obtained by projecting the incoming GWP on incoming plane waves $\exp(-ikx)$ and the scattered wave function on outgoing plane waves $\exp(ikx)$, respectively.

In Sec. II, we have derived the equations of motion for the present problem using the Hermite correction method. Models used in the calculations are presented in Sec. III. The essential steps of initialization, propagation, and projection procedures are described in Sec. IV. Finally, in Sec. V, we have discussed the transition probabilities for the two models obtained by our method and compared with exact quantum results.

II. THE HERMITE-CORRECTION METHOD FOR MULTISURFACE SYSTEMS

The general form of the matrix equation for a one-dimensional multisurface system in the diabatic representation can be expressed as

$$i\hbar \frac{\partial}{\partial t} \Psi(x,t) = [\hat{T}_x + \hat{V}(x)] \Psi(x,t), \quad (1)$$

where

^{a)}Electronic mail: gdb@moldyn.ki.ku.dk

$$\hat{\mathbf{T}}_x \equiv \hat{T}_x \begin{pmatrix} 1 & 0 & \cdot & \cdot & 0 & 0 \\ 0 & 1 & \cdot & \cdot & 0 & 0 \\ \cdot & \cdot & \cdot & \cdot & \cdot & \cdot \\ \cdot & \cdot & \cdot & \cdot & \cdot & \cdot \\ 0 & 0 & \cdot & \cdot & 1 & 0 \\ 0 & 0 & \cdot & \cdot & 0 & 1 \end{pmatrix}, \quad (2)$$

$$\hat{\mathbf{V}}(x) \equiv \begin{pmatrix} \hat{V}_{11}(x) & \hat{V}_{12}(x) & \cdot & \cdot & \cdot & \hat{V}_{1k}(x) \\ \hat{V}_{21}(x) & \hat{V}_{22}(x) & \cdot & \cdot & \cdot & \hat{V}_{2k}(x) \\ \cdot & \cdot & \cdot & \cdot & \cdot & \cdot \\ \cdot & \cdot & \cdot & \cdot & \cdot & \cdot \\ \cdot & \cdot & \cdot & \cdot & \cdot & \cdot \\ \hat{V}_{k1}(x) & \hat{V}_{k2}(x) & \cdot & \cdot & \cdot & \hat{V}_{kk}(x) \end{pmatrix}, \quad (3)$$

and

$$\Psi(x, t) \equiv \begin{pmatrix} \psi_1(x, t) \\ \psi_2(x, t) \\ \cdot \\ \cdot \\ \cdot \\ \psi_k(x, t) \end{pmatrix}, \quad (4)$$

with $\Psi^\dagger(x, t)\Psi(x, t) = 1$ at all times t .

The kinetic energy operator, $\hat{T}_x = \hat{p}_x^2/(2\mu)$, and the diagonal elements of the matrix in Eq. (3) represent potential energy operators for different surfaces where off-diagonal elements define the coupling among them. The l th element of the wave function matrix in Eq. (4) is the wave function for the l th surface. It can be expanded it as

$$\psi_l(x, t) = \sum_n c_{nl}(t) \Phi_{nl}(x, t). \quad (5)$$

The basis functions, $\Phi_{nl}(x, t)$, used in Eq. (5) are the Gauss–Hermite basis functions defined by

$$\Phi_{nl}(x, t) = \pi^{1/4} \exp\left(\frac{i}{\hbar}(\gamma_l(t) + p_l(t)(x - x_l(t)) + \text{Re } A_l(t)(x - x_l(t))^2)\right) \phi_n(\xi_l(t)), \quad (6)$$

where

$$\phi_n(\xi_l(t)) = \frac{1}{\sqrt{n!2^n\sqrt{\pi}}} \exp(-\xi_l(t)^2/2) H_n(\xi_l(t)), \quad (7)$$

with

$$\xi_l(t) = \sqrt{\frac{2 \text{Im } A_l(t)}{\hbar}} (x - x_l(t)), \quad (8)$$

and H_n are the Hermite polynomials. The basis set, $\Phi_{nl}(x, t)$, form an orthonormal set, i.e.,

$$\int dx \Phi_{nl}^*(x, t) \Phi_{ml}(x, t) = \delta_{nm}^l, \quad (9)$$

which is ensured by

$$\text{Im } \gamma_l(t) = -\frac{\hbar}{4} \ln\left(\frac{2 \text{Im } A_l(t)}{\pi \hbar}\right), \quad (10)$$

at all times t .

The first part (the Gauss part) plays an important role by generating the equations of motion driving the basis set along in space.

If we include only one basis function in the expansion (5) for each surface l , and substitute in Eq. (1), we can arrive at the following set of equations:

$$i\hbar \dot{c}_{0l} = \frac{p_l^2(t)}{2\mu} c_{0l} + \sum_k V_{0l,0k}(t) c_{0k}, \quad (11)$$

$$\dot{p}_l(t) = -V'_{\text{eff},l}, \quad (12)$$

$$\dot{x}_l(t) = \frac{p_l(t)}{\mu}, \quad (13)$$

$$\dot{A}_l(t) = -\frac{2}{\mu} A_l(t)^2 - \frac{1}{2} V''_{\text{eff},l}, \quad (14)$$

$$\dot{\gamma}_l(t) = \frac{p_l^2(t)}{\mu} + \frac{i\hbar A_l(t)}{\mu}, \quad (15)$$

where

$$V_{0l,0k}(t) = \int dx \Phi_{0l}^*(x, t) V_{lk}(x) \Phi_{0k}(x, t), \quad (16)$$

$$V'_{\text{eff},l} = \sum_k \int dx \Phi_{0l}^*(x, t) \frac{d}{dx} V_{lk}(x) \Big|_{x=x_l(t)} \Phi_{0k}(x, t), \quad (17)$$

$$V''_{\text{eff},l} = \sum_k \int dx \Phi_{0l}^*(x, t) \frac{d^2}{dx^2} V_{lk}(x) \Big|_{x=x_l(t)} \Phi_{0k}(x, t), \quad (18)$$

i.e., we have obtained a set of coupled equations in the expansion coefficients and equations for the motion of the center of the basis set [Eqs. (12) and (13)] and for the width and phase of the wave packet [Eqs. (14) and (15)]. Equations (11)–(13) and (16) and (17) are what is known as the primitive quantum classical (PQC) equations in which the trajectory is driven by a mean field potential. For the situation we are considering with nonadiabatic transitions and interference effects playing a role, we do not expect these equations to be adequate (see also Ref. 19).

However, we are now in a position that we can formulate rigorous classical path equations within the MCSCF framework. The wave functions for each surface are expanded in the Gauss–Hermite basis set as shown in Eq. (5) and substituted in the matrix Eq. (1). At this point, it is important to note that we use the following equations in the derivation:

$$\frac{d}{dt} x_l(t) = p_l(t)/\mu, \quad (19)$$

$$\frac{d}{dt} \text{Im } A_l(t) = -\frac{4}{\mu} \text{Re } A_l(t) \text{Im } A_l(t), \quad (20)$$

$$\frac{d}{dt} \text{Im } \gamma_l(t) = \frac{\hbar}{\mu} \text{Re } A_l(t). \quad (21)$$

This is already suggested by inspection of Eqs. (13)–(15) in the PQC method. These equations are now used to ensure the classical path picture, i.e., the center of the wave packet follows classical equations of motion governed by Eqs. (19) and (24) or Eqs. (12) and (13). After some simplifications, one can derive the following set of coupled equations for the expansion coefficients, c_{mk} :

$$\begin{aligned} i\hbar \dot{c}_{nl} = & \left\{ 2n \frac{\hbar \text{Im } A_l(t)}{\mu} + \frac{p_l^2(t)}{2\mu} - \frac{\hbar(n + (1/2))}{4 \text{Im } A_l(t)} V''_{\text{eff},l} \right\} c_{nl} \\ & + \sum_{mk} V_{nl,mk}(t) c_{mk} - \frac{V'_{\text{eff},l}}{2} \sqrt{\frac{\hbar}{\text{Im } A_l(t)}} \\ & \times \{ \sqrt{n} c_{n-1,l} + \sqrt{n+1} c_{n+1,l} \} - \frac{1}{8} V''_{\text{eff},l} \frac{\hbar}{\text{Im } A_l(t)} \\ & \times \{ \sqrt{n(n-1)} c_{n-2,l} + \sqrt{(n+1)(n+2)} c_{n+2,l} \}, \end{aligned} \quad (22)$$

where

$$V_{nl,mk}(t) = \int dx \Phi_{nl}^*(x,t) V_{lk}(x) \Phi_{mk}(x,t),$$

and the rigorous expressions for $V'_{\text{eff},l}$ and $V''_{\text{eff},l}$ are derived using the Dirac–Frenkel¹⁷ variational principle. Thus, we can write the following integral equation using matrix Eq. (1):

$$\begin{aligned} & \int dx (-i\hbar \Psi^*(x,t) - \hat{\mathbf{H}}(x, p_x) \Psi^*(x,t)) \\ & \times (i\hbar \Psi(x,t) - \hat{\mathbf{H}}(x, p_x) \Psi(x,t)), \end{aligned} \quad (23)$$

and minimize with respect to $\dot{p}_l(t)$ and $\text{Re } \dot{A}_l(t)$. After some algebraic manipulations (!), one can get²

$$\dot{p}_l(t) = -V'_{\text{eff},l}, \quad (24)$$

$$\text{Re } \dot{A}_l(t) = -\frac{2}{\mu} (\text{Re } A_l(t)^2 - \text{Im } A_l(t)^2) - \frac{1}{2} V''_{\text{eff},l}, \quad (25)$$

with

$$V'_{\text{eff},l} = \frac{\begin{vmatrix} V_1^l & S_l^{(3)} - X_{11}^l \\ V_2^l & S_l^{(4)} - X_{22}^l \end{vmatrix}}{\begin{vmatrix} S_l^{(2)} - X_{11}^l & S_l^{(3)} - X_{12}^l \\ S_l^{(3)} - X_{21}^l & S_l^{(4)} - X_{22}^l \end{vmatrix}}, \quad (26)$$

and

$$\frac{1}{2} V''_{\text{eff},l} = \frac{\begin{vmatrix} S_l^{(2)} - X_{11}^l & V_1^l \\ S_l^{(3)} - X_{22}^l & V_2^l \end{vmatrix}}{\begin{vmatrix} S_l^{(2)} - X_{11}^l & S_l^{(3)} - X_{12}^l \\ S_l^{(3)} - X_{21}^l & S_l^{(4)} - X_{22}^l \end{vmatrix}}, \quad (27)$$

where

$$V_1^l = \sum_{nmk} c_{nl}^* c_{mk} \left(V_{nl,mk}^{(1)} - \sum_p S_{nl,pl}^{(1)} V_{pl,mk}^{(0)} \right), \quad (28)$$

$$V_2^l = \sum_{nmk} c_{nl}^* c_{mk} \left(V_{nl,mk}^{(2)} - \sum_p S_{nl,pl}^{(2)} V_{pl,mk}^{(0)} \right), \quad (29)$$

$$V_{nl,mk}^{(l)} = \int \Phi_{nl}^*(x,t) V_{lk}(x) (x - x_l(t))^l \Phi_{mk}(x,t) dx, \quad (30)$$

$$X_{IJ}^l = \sum_{nm} c_{nl}^* c_{ml} \sum_p S_{nl,pl}^{(l)} S_{pl,ml}^{(J)}, \quad (31)$$

$$S_{nl,ml}^{(l)} = \int dx \Phi_{nl}^*(x,t) (x - x_l(t))^l \Phi_{ml}(x,t), \quad (32)$$

$$S_l^I = \sum_{nm} c_{nl}^* c_{ml} S_{nl,ml}^I. \quad (33)$$

We notice that each surface has its own basis set, the center of which is governed by a trajectory propagated by effective quantum forces given by Eq. (26). These trajectories (one for each surface) moves the basis functions according to the dynamics of the system.

The integrals in Eq. (32) have analytical closed form expressions because of the use of the Hermite basis. In the present case, due to the simple form of the model potentials, integrals in Eq. (30) also have closed form expressions. But, in case of real systems, one can expand the potential energy function in terms of plane waves to get analytical expressions and thereby reduce the numerical cost.

III. THE MODELS

We have tested our proposed method on two one-dimensional two-state systems,¹⁶ both of them are expressed in the diabatic representation. The first is called the “simple avoided crossing” model. It is defined by

$$\begin{aligned} V_{11} &= A[1 - \exp(-Bx)], x > 0, \\ V_{11} &= -A[1 - \exp(Bx)], x < 0, \\ V_{22} &= -V_{11}(x), \\ V_{12} &= V_{21} = C \exp(-Dx^2), \end{aligned} \quad (34)$$

and the second is the “dual avoided crossing” model, in which

$$\begin{aligned} V_{11} &= 0, \\ V_{22} &= -A[1 - \exp(-Bx^2)] + E_0, \\ V_{12} &= V_{21} = C \exp(-Dx^2). \end{aligned} \quad (35)$$

The second model can produce quantum interference effects (Stueckelberg oscillations) in the excitation probabilities. The parameters used in the above models are given in Table I.

IV. INITIALIZATION, PROPAGATION, AND PROJECTION

In all calculations, we have represented the initial ground state wave function by a Gaussian wave packet (GWP) where the center of the wave packet is localized in

TABLE I. Potential parameters and other datas used in calculations. 1 \hat{e} = 100 KJ/mol and 1 τ = 10^{-14} s.

| Parameter | Value | Unit |
|--------------------|--------|--|
| μ | 1.0893 | amu |
| Im $A_1(t=0)$ | 0.5 | amu τ^{-1} |
| Re $A_1(t=0)$ | 0.0 | amu τ^{-1} |
| Re $\gamma_1(t=0)$ | 0.0 | $\tau \text{ \AA}^{-2} \text{ amu}^{-1}$ |
| Model I: | | |
| A | 0.2624 | \hat{e} |
| B | 3.0236 | \AA^{-1} |
| C | 0.1312 | \hat{e} |
| D | 3.5711 | \AA^{-2} |
| Model II: | | |
| A | 2.6243 | \hat{e} |
| B | 0.9999 | \AA^{-2} |
| E_0 | 1.3121 | \hat{e} |
| C | 0.3936 | \hat{e} |
| D | 0.2143 | \AA^{-2} |

the negative region ($-x_1(t_0)$) of the x coordinate and the wave function matrix, $\Psi(x, t) = (\psi_0^{\text{GWP}})$. Parameters used in GWP are given in Table. I.

The propagation has been carried out using 30 Gauss–Hermite basis functions as shown in Eq. (5) on each surface and is continued until the centers of the wave packets, $x_1(t)$ and $x_2(t)$ for the lower (l) and upper (u) surfaces, respectively, are far from the intersection region of the surfaces.

For both the models, we are interested in calculating the probability of transmission (P_{tr}^l) and reflection (P_{re}^l) on the lower electronic state and the probability for transmission (P_{tr}^u) on the upper state at different energies. At a particular energy, we have propagated the equations sufficiently in time to make sure that the wave functions are free of the interaction region and then integrated over space to get the above mentioned probabilities

$$\begin{aligned}
 P_{tr}^l &= \int_{x_{\min}}^{\infty} dx \psi_l(x), \\
 P_{re}^l &= \int_{-\infty}^{x_{\max}} dx \psi_l(x), \\
 P_{tr}^u &= \int_{x_{\min}}^{\infty} dx \psi_u(x),
 \end{aligned} \tag{36}$$

where before x_{\min} and after x_{\max} in the x coordinate the wave functions and interaction potentials are practically zero.

The probabilities obtained by averaging over certain regions as in Eqs. (36) are average probabilities corresponding to the mean value of the momentum of the GWP. In order to obtain properly energy resolved quantities we need to project the wave function on incoming and outgoing plane waves and take the ratio of outgoing and incoming fluxes at that particular energy. Thus we have

$$P_{tr}^l(E) = \frac{k_{\text{out}}/\mu |1/\sqrt{2\pi} \int_{-\infty}^{\infty} \psi_l(x, t) \exp(ik_{\text{out}}x) dx|^2}{k_{\text{in}}/\mu |1/\sqrt{2\pi} \int_{-\infty}^{\infty} \psi_{\text{GWP}}(x, t_0) \exp(ik_{\text{in}}x) dx|^2},$$

$$P_{re}^l(E) = \frac{k_{\text{out}}/\mu |1/\sqrt{2\pi} \int_{-\infty}^{\infty} \psi_l(x, t) \exp(-ik_{\text{out}}x) dx|^2}{k_{\text{in}}/\mu |1/\sqrt{2\pi} \int_{-\infty}^{\infty} \psi_{\text{GWP}}(x, t_0) \exp(ik_{\text{in}}x) dx|^2}, \tag{37}$$

$$P_{tr}^u(E) = \frac{k_{\text{out}}/\mu |1/\sqrt{2\pi} \int_{-\infty}^{\infty} \psi_u(x, t) \exp(ik_{\text{out}}x) dx|^2}{k_{\text{in}}/\mu |1/\sqrt{2\pi} \int_{-\infty}^{\infty} \psi_{\text{GWP}}(x, t_0) \exp(ik_{\text{in}}x) dx|^2},$$

where k_{in} , k_{out} and total energy E are related by the equation given below

$$E = E_{\alpha} + \frac{\hbar^2 k_{\text{in}}^2}{2\mu} = E_{\beta} + \frac{\hbar^2 k_{\text{out}}^2}{2\mu}, \tag{38}$$

with E_{α} and E_{β} are the potential energies for the channels α and β , respectively. In an energy range where the probability varies little with the energy the difference between the properly energy resolved and the average probabilities is not significant. But near the threshold we need to use Eq. (37).

V. RESULTS AND DISCUSSION

At a particular energy and for each system, the ground state wave function, a GWP was localized in the asymptotic negative x region with a positive momentum and then propagated until the wave functions were completely free of the interaction region. Finally the transition probabilities are calculated by using Eq. (37) at low energies and Eq. (36) at high energies.

In Figs. 1(a)–1(c), we have displayed our calculated numbers obtained by the Hermite correction method using the simple avoided crossing model and compared with quantum results. At low energies ($k < 9$ a.u.), the plane wave projection techniques were used to get probabilities for a range of energies using the initial and final wave functions at a particular energy ($k = 7$ a.u.). This procedure improves the probabilities at very low energies ($k = 1$ –5 a.u.) dramatically with respect to the direct space integration procedure. But, for high energies ($k > 9$ a.u.), we have propagated the system at a particular energy and integrated the final wave function over space to obtain probabilities at that energy. As the mass of the system is equal to that of a hydrogen atom, one might expect tunneling to be important. However, quantum as well as our results indicate that tunneling gives very little contribution to probabilities even at low energies ($k < 4.5$ a.u.). If the kinetic energy ($5 < k < 9$) of the system is below the asymptotic energy of the upper surface, there is no final population on the upper surface while the transmission probability on the lower surface increases like a step function. At high energies ($k > 9$ a.u.), the transmission probability on the upper surface increases and it decreases gradually on the lower surface. Thus, at all energies, agreement between our numbers obtained by using the Gauss–Hermite basis set and the quantum results is impressive.

We have presented our and the quantal results for the model dual avoided crossing in Figs. 2(a)–2(c). As in the case of the earlier model, probabilities at low energies are calculated by using plane wave projection technique [Eq. (37)] and at high energies by integrating the final wave function over space [Eq. (36)]. Results obtained by the Gauss–Hermite method are in good agreement with the quantal values at all energies. Most interestingly, the method can

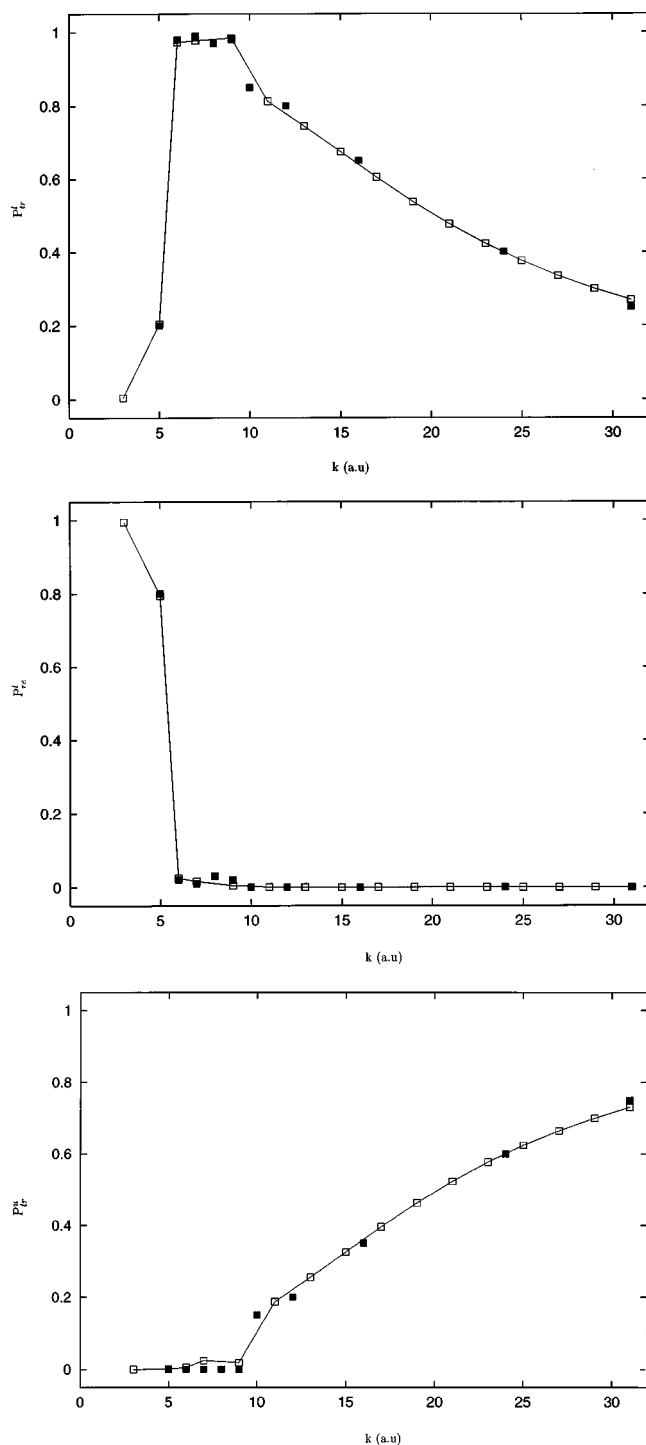


FIG. 1. (a) Probability of transmission (P_{tr}^l) on the lower electronic state, (b) probability of reflection (P_{re}^l) on the lower state, and (c) probability of transmission (P_{tr}^u) on the upper state are shown as a function of wave number, k (a.u.), for the Simple avoided crossing model. In each figure, open boxes with solid lines are results from present calculations and filled boxes are quantum mechanical results from (Ref. 16).

reproduce the strong Stuckelberg oscillations, a quantum interference effect, present in the model. The position as a function of $\log(E)$ of the peaks and valleys in the transmission probabilities on the ground and upper surfaces almost coincide with the quantum ones. The reflection probabilities

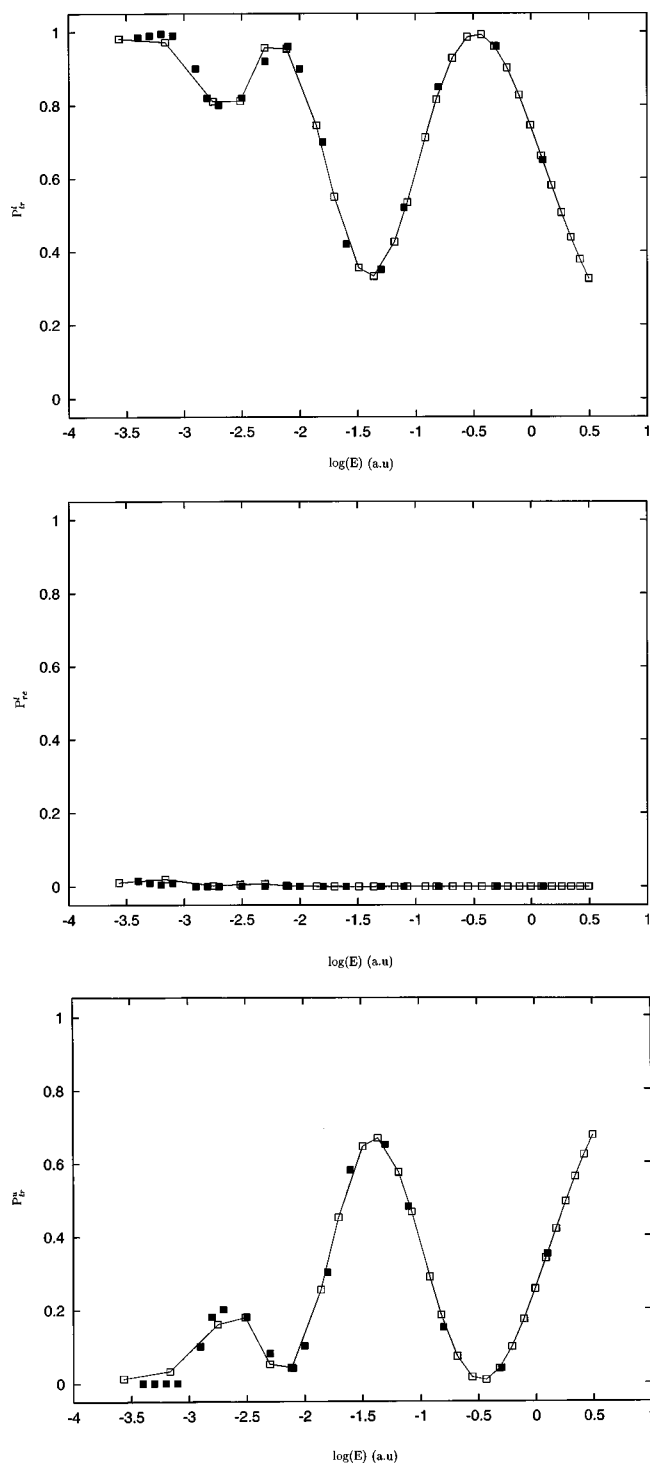


FIG. 2. (a) Probability of transmission (P_{tr}^l) on the lower electronic state, (b) probability of reflection (P_{re}^l) on the lower state, and (c) probability of transmission (P_{tr}^u) on the upper state are displayed as a function of, $\log(E)$ (a.u.), for the Dual avoided crossing model. Symbols are the same as in Fig. 1.

on the lower surface remain zero at all energies as in the quantum mechanical calculations.

VI. CONCLUSION

We have shown that the Gauss–Hermite method can be used to obtain accurate transition probabilities for a system

involving more than one electronic state. In the present calculations we have used 30 Gauss–Hermite basis functions on each surface and obtained probabilities by using the projection techniques as applied in time dependent quantum mechanics. No overlap between various sets of basis functions need to be calculated unless a multitrajectory approach with basis sets centered around individual trajectories on the same potential energy surface are introduced.²

If, we formulate equations of motion using only one basis function (GWP), the quantities as $\dot{p}_i(t)$, $\dot{x}_i(t)$ are driven by classical forces obtained as derivatives of an effective potential, whereas with the increased basis in Eq. (5), it is possible to show that these quantities are driven by “quantum forces” which cannot be obtained as derivatives of a potential, i.e., they are not classical in the sense of “Newton.”¹⁸ Thus, the Hermite correction method can accordingly offer a systematic passage from classical mechanics to quantum mechanics and can also be used to predict how classical a given degree of freedom is. This makes the basis set convenient to use for incorporating classical mechanics in part of the system—keeping a quantum description of the remaining. However, since integrals over basis functions have to be evaluated, the quantum part of the method is time-consuming unless special techniques are developed. We have introduced a Fourier transform method¹⁸ in order to facilitate the evaluation of the matrix elements. An even faster methodology is presently being explored—namely to build a time dependent discrete variable representation scheme around the trajectories. With this latter development we expect the scheme to be very competitive.

ACKNOWLEDGMENTS

This research was supported by the Danish Natural Research Council and the EU TMR Grant No. ERBFM-RXCT960088.

- ¹G. D. Billing, J. Chem. Phys. **99**, 5849 (1993); Int. Rev. Phys. Chem. **13**, 309 (1994).
- ²G. D. Billing, J. Chem. Phys. **107**, 4286 (1997).
- ³G. D. Billing, *Encyclopedia of Computational Chemistry*, edited by H. F. Schaefer III (Wiley, New York, 1998).
- ⁴E. J. Heller, J. Chem. Phys. **64**, 63 (1976); D. Huber and E. J. Heller, *ibid.* **89**, 4752 (1988).
- ⁵S. I. Sawada, R. Heather, B. Jackson, and H. Metiu, J. Chem. Phys. **83**, 3009 (1985); R. B. Gerber, R. Kosloff, and M. Berman, Comput. Phys. Rep. **5**, 59 (1986).
- ⁶T. J. Martinez, M. Ben-Nun, and R. D. Levine, J. Phys. Chem. **100**, 7884 (1996).
- ⁷R. B. Gerber, V. Buch, and M. A. Ratner, J. Chem. Phys. **77**, 3022 (1982); H.-D. Meyer, U. Manthe, and L. S. Cederbaum, Chem. Phys. Lett. **165**, 73 (1990); N. Makri and W. H. Miller, J. Chem. Phys. **87**, 5781 (1987).
- ⁸S. Adhikari and G. D. Billing, Chem. Phys. **238**, 69 (1998); Chem. Phys. Lett. (in press); Chem. Phys. Lett. (submitted).
- ⁹H.-D. Meyer, Chem. Phys. **61**, 365 (1981).
- ¹⁰R. D. Coalson and M. Karplus, Chem. Phys. Lett. **90**, 301 (1982).
- ¹¹K. B. Möller and N. E. Henriksen, J. Chem. Phys. **105**, 5037 (1996).
- ¹²K. G. Kay, Phys. Rev. A **46**, 1213 (1992); J. Chem. Phys. **91**, 170 (1989).
- ¹³S.-Y. Lee and E. J. Heller, J. Chem. Phys. **76**, 3035 (1982).
- ¹⁴J. Kucar and H.-D. Meyer, J. Chem. Phys. **90**, 5566 (1989).
- ¹⁵D. J. Tannor, A. Besprozvannaya, and C. J. Williams, J. Chem. Phys. **96**, 2998 (1992).
- ¹⁶J. C. Tully, J. Chem. Phys. **93**, 1061 (1990).
- ¹⁷P. A. M. Dirac, Proc. Cambridge Philos. Soc. **26**, 376 (1930).
- ¹⁸G. D. Billing, J. Chem. Phys. **110**, 5526 (1999).
- ¹⁹Z. Kotler, E. Neria, and A. Nitzan, Comput. Phys. Commun. **63**, 243 (1991).